

REVIEW ARTICLE

Surface Premelting of Ice

Yimin Li and Gabor A. Somorjai

Department of Chemistry and Lawrence Berkeley National Laboratory, Berkeley, California 94720

Received: February 8, 2007; In Final Form: April 13, 2007

In this review, we summarize the available experimental data from recently developed molecular level techniques on the surface structure, surface premelting layer thickness, and friction of ice. We conclude that surface premelting of ice is responsible for the unique surface properties of the important substance.

Introduction

It is well-known that the unusual slipperiness of the ice surface is due to a lubricating layer of water on the ice surface. There are three proposed mechanisms for the formation of this layer: pressure melting, frictional heating, and intrinsic premelting.^{1–3} The conventional explanation, pressure melting, was suggested by James Thomson in 1850 as a consequence of the higher density of liquid water relative to ice. Frictional heating, proposed by Bowden and Hughes in 1939 is another commonly accepted explanation.⁴ Intrinsic premelting of the ice surface is a mechanism for lubricating ice which has been subjected to intensive experimental and theoretical studies for more than a century.^{1,3,5,6}

Intrinsic premelting is the phenomenon where a thin layer of water-like liquid is present on the ice surface without heating from other contact surface at a temperature below the bulk melting point for a given pressure. In 1842, Michael Faraday first suggested the existence of a premelting layer after he observed the regelation of ice. In the earlier days, the experimental proof for the premelting layer was difficult because experiments such as regelation of ice⁷ could not completely rule out the pressure effect due to the contact of two surfaces. More convincing evidence was provided by an X-ray diffraction experiment in 1987.⁸ In the modern perspective, surface premelting is a direct consequence to the abrupt termination of the strong bonding environment for the surface water molecules. The lowering of the surface free energy is the driving force for

the formation of the premelting layer at a temperature much lower than the bulk melting point.⁹

In addition to its role in lowering the friction on ice, striking environmental consequences of the premelting layer on ice have been suggested recently which motivate further research efforts to understand the properties of the premelting layer at the molecular level.^{1,3} The central questions needed to be addressed include the following: What is the surface molecular structure of ice at very low temperature (~ 100 K)? How does it change with the temperature increase to form a premelting layer? What are the effects of the surface orientation, impurities, external load, and friction heating on the formation and properties of the premelting layer? What is the role of the premelting layer in lowering the friction of the ice surface?

In this paper, we review the current state of understanding of the formation and properties of the premelting layer on the ice surface. We first discuss the surface molecular structural properties of ice. Then, we review recent studies on the temperature dependence of the layer thickness and discuss possible factors that cause large variations in the different experimental results. Finally, we review friction studies using atomic force microscopy on the ice surface. The goal of this review is to focus on molecular studies of the ice surface and to stimulate future research in order to understand how the unique molecular structure of the premelting layer affects the frictional properties of the ice surface.

Structure of the Ice Surface. Structural information is a prerequisite for understanding the unique physical properties

of the ice surface at the molecular level. Structural studies tell about the bonding environment and the orientation of surface molecules, and they sometimes give information about the molecular disorder at the surface due to the finite temperature. Table 1 lists three experimental techniques used in surface structural studies of ice.

Using the low-energy electron diffraction (LEED) technique, total-energy calculations, and molecular dynamics simulations, Materer et al. studied the surface of an ultrathin ice (0001) film (~ 10 Å) grown on a Pt(111) substrate at 90 K.^{10,11} The results suggested that the ice (0001) surface is terminated as a full bilayer instead of a half bilayer (see Figure 1). This surface structure was later observed on a thicker ice film by a helium atom scattering experiment at 30 K.^{12,13} The theoretical analysis of the LEED result also suggested strongly vibrating water molecules exist in the top half of the outermost bilayer. The surface root-mean-square (rms) vibrational amplitude is 0.25–0.33 Å in contrast to that of 0.10 Å in the bulk.

As shown in Figure 1, there are dangling or “free” O–H bonds sticking out of the ice surface. The orientation disorder of these dangling O–H bonds has been investigated by sum-frequency generation (SFG) vibrational spectroscopy in the temperature range of 173–271 K.^{14,15} The SFG is sensitive to the stretching motion of the dangling O–H bond perpendicular to the ice surface. The orientation disorder can reduce the intensity of the SFG signal of free O–H bonds. The results of SFG (see Figure 2) showed that the disorder of free O–H bonds becomes detectable as the temperature approaches about 200 K and is enhanced by the further temperature increase.

The results of SFG also suggested that the structural ordering decreases continuously from the solid phase to the ice surface across the premelting layer. This suggestion is compatible with the results from glancing-angle X-ray scattering and proton channeling but is inconsistent with a simple model which assumes the premelting layer as a uniform water layer.^{16,17}

Ikeda-Fukazawa and Kawamura performed a molecular dynamics study of the ice (0001) surface with an atom–atom potential model.¹⁸ Their results (see Figures 3 and 4) fully support experimental observations of the large vibrational and rotational motion of water molecules in the top layer at temperatures far below the bulk melting point and the continuous variation of structural ordering across the premelting layer.

Thickness of the Premelting Layer. A variety of surface science techniques have been employed to determine the temperature dependence of the premelting layer thickness.^{8,16,17,19–28} Some of them are listed Table 2. All of these experimental studies confirm the existence of the premelting layer at temperatures below the bulk melting point. It is commonly believed that the onset premelting temperature is around 243 K. The thickness increases very fast as the temperature approaches the bulk melting point. The premelting layer does not behave exactly like supercooled liquid water, so it is also referred to as a quasi-liquid layer. However, these experiments do not agree on the temperature dependence of the layer thickness. As shown in refs 2 and 24, the thickness measurements from different experimental approaches can vary as much as 2 orders of magnitude at a given temperature.

Different techniques are based on different physical properties of the premelting layer to measure the thickness (as shown in Table 2), so their sensitivities are different. Generally, the techniques detecting molecular structural changes at the surface are more sensitive and usually suggest lower onset temperature for premelting. Those techniques that sample bulk properties

Yimin Li received his B.S. in electronic engineering from Shanghai University, China, in 1992 and his Ph.D. in physical chemistry from New York University, New York, in 2003. Currently, He is a post-doctoral researcher in the Department of Chemistry at the University of California, Berkeley.



Gabor A. Somorjai received his B.S. in chemical engineering from the Technical University, Hungary, in 1956 and his Ph.D. in chemistry from the University of California, Berkeley, in 1960. After graduation, he joined the IBM research staff in New York, where he remained until 1964. Since then he has been a member of the faculty in the Department of Chemistry at the University of California, Berkeley. He is also a Faculty Senior Scientist in the Materials Sciences Division and Program Leader of the Surface Science and Catalysis Program at the Center for Advanced Materials, Lawrence Berkeley National Laboratory. His research interests lie in the fields of surface chemistry, heterogeneous catalysis, and solid state chemistry.

of the premelting layer usually work well at the temperature relatively close to the bulk melting point when a thicker film is formed.

Ice sample preparation can also cause uncertainties in the measured thickness of the premelting layer. It is demonstrated by optical reflection experiments that temperature dependencies of the layer thickness on the basal and the prismatic surface of ice can be totally different.²³ It is difficult to grow a crystalline ice with a large surface area of well-defined orientation, so some experiments were performed on thin films of ice or on polycrystalline ice surfaces (Table 2).

Surface contamination is thought to be a major cause of uncertainty in different experimental measurements. A theoretical analysis by J. Wettlaufer suggested that the layer thickness can be extremely sensitive to small impurity concentrations.²⁹ In the optical reflection experiment, M. Elbaum et al. observed that introducing a small amount of air to the ice surface can significantly promote surface premelting.²³ In a recent experiment, H. Bluhm et al. have used the X-ray photoemission spectroscopy (XPS) to quantify the degree of hydrocarbon contamination on different samples of the ice surface and the near-edge X-ray absorption fine-structure spectroscopy (NEXAFS) to measure the premelting layer thickness at different temperatures for different samples.²⁰ Their results (see Figure 5) clearly show the important role of surface contamination in enhancing the extent of premelting. A recent molecular dynamics study further demonstrates how foreign ions such as NO_3^- , Cl^- , Na^+ , and H^+ in the ice surface can reduce the inhibition of the librational vibrations of surface water molecules and consequently increase the premelting layer thickness.³⁰

Friction of the Ice Surface. At a macroscopic level, the coefficient of friction on ice is about 1 order of magnitude lower than on other solids. However, it is not constant and depends on many factors such as sliding speed, temperature, asperities

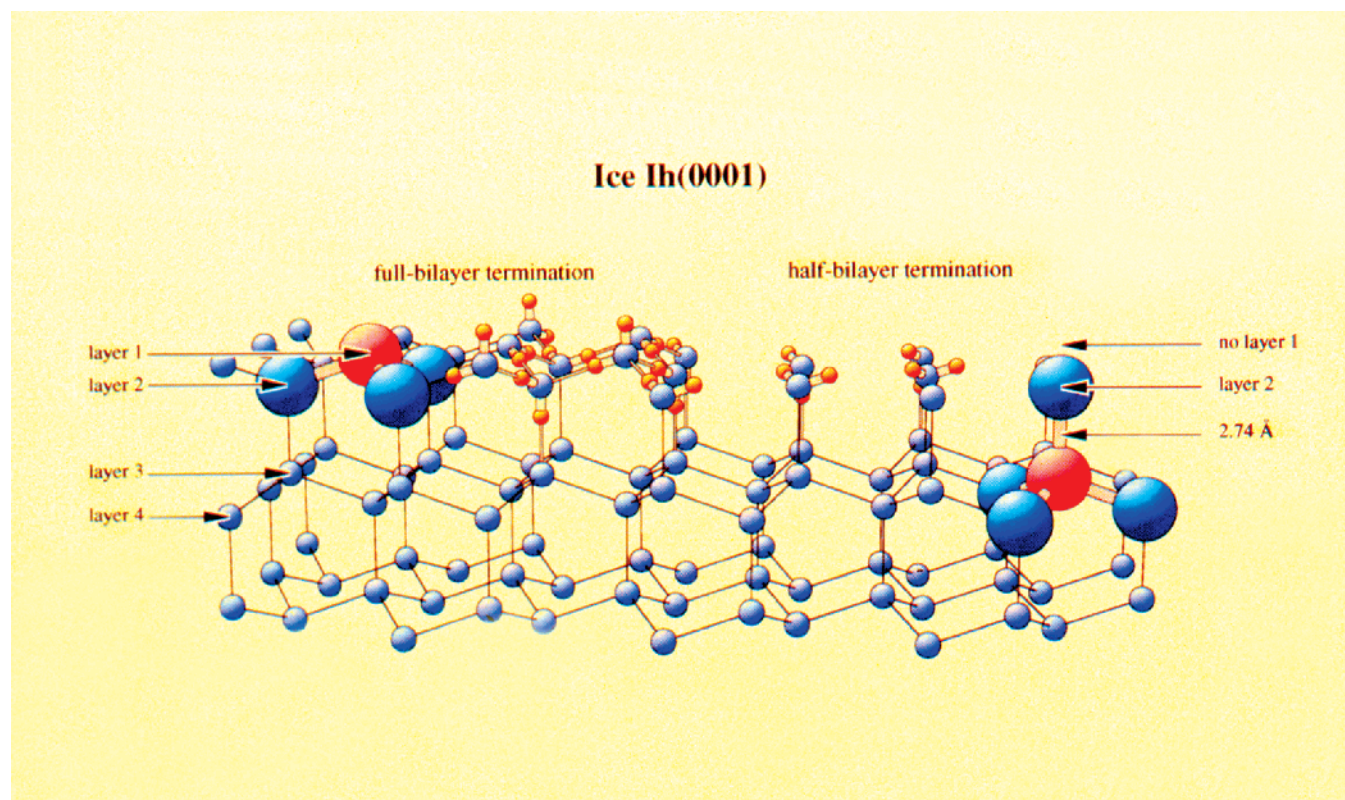


Figure 1. Perspective grazing view of the ice Ih (0001) surface, showing two ideal terminations on top: full-bilayer termination at left (layer 1 is present) and half-bilayer termination at right (layer 1 is absent). Molecules in layer 1 are found to have enhanced vibrational amplitudes, making them invisible in LEED. Middle-size atoms are oxygens, with some hydrogens included as small atoms with assumed bulk-like positions and randomness to form H₂O molecules (covalent bonds are drawn medium thick and hydrogen bonds medium thin). Large spheres represent complete H₂O molecules, emphasizing their tetrahedral bulk-like bonding arrangement (from ref 10).

of the contact surface, and the load.^{31,32} The coefficient of friction on ice decreases as the sliding speed increases with the other parameters fixed. At very low sliding speed, the coefficient of friction on ice is extremely high. For example, Persson found that, at speeds around 10⁻⁷ m/s, glass and granite on ice are 0.3 and 0.9, respectively.³² At the macroscopic level, this phenomenon can be explained as the high-speed promotes the friction heating on the ice surface. At a microscopic level, the high-speed means that the asperities of the slider has less time to squeeze out the lubricating water layer in the contact areas and to cause the large plastic deformation on the ice surface. Thus, the friction is lower at higher speed.

In general, a temperature increase can lower the coefficient of friction on ice since the thickness of the premelting layer is greater at higher temperatures.^{31,33} However, it was found experimentally that the optimum temperature for speed skating is around -7 °C with a coefficient of friction of 0.0046.³⁴ This shows that, as the temperature increases to some extent, the ice surface becomes too soft, and then the plastic deformation of the ice surface can cause a significant increase of the real contact

area between the skate and the ice surface.^{35,36} At the same load, the increase of the real contact area results in a greater adhesive force and consequently a greater friction force.

The deformation of polycrystalline ice surfaces has been studied by microscopic indentation with atomic force microscope (AFM) tips.³⁷⁻³⁹ A typical force curve taken by Pittenger et al. is shown in Figure 6. Their study suggested that the ice surface undergoes plastic deformation immediately upon contact with the tip. The estimated yield strengths are 14 MPa at -10.4 °C and 20 MPa at -15.1 °C which are much smaller than Young's modulus of the bulk ice. The increase of contact area due to the depression increases the adhesive force between the tip and the ice surface. To elucidate the mechanism for the formation of plastic flow during the plastic deformation, indentations with different approaching speeds (see Figure 7) were performed. Butt et al. suggested that the tip penetration speed was limited by the rate of the melting process induced by the pressure under the tip.³⁸ However, Pittenger et al. argued that, in the cases with lower approaching speed, the pressure under the tip is not high enough to initiate the melting process.³⁹ Thus, there should be

TABLE 1: Several Surface Techniques for Surface Structural Studies of Ice

surface science technique	description
low-energy electron diffraction ¹⁰	Monoenergetic electrons below ~500 eV are elastically back-scattered from a surface and detected as a function of energy and angle.
helium atom scattering ¹²	Helium atoms with energies of about 7–100 meV are back-scattered from a surface. Analysis of the angular distribution of helium atoms backscattered from a surface yields the corrugation function of the surface which in turn reveals the surface structure.
sum-frequency generation vibrational spectroscopy ¹⁴	A surface is illuminated by two lasers. One of the lasers has a tunable frequency. Surface molecules are vibrationally excited by the two lasers through nonlinear optical processes.

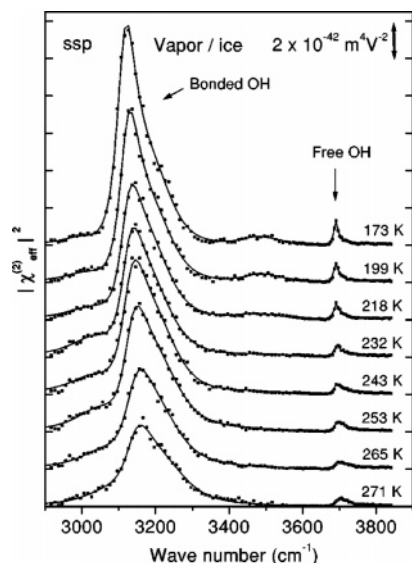


Figure 2. SFG spectra of the vapor/ice (0001) interface at various temperatures. The polarization combination is ssp (from ref 15).

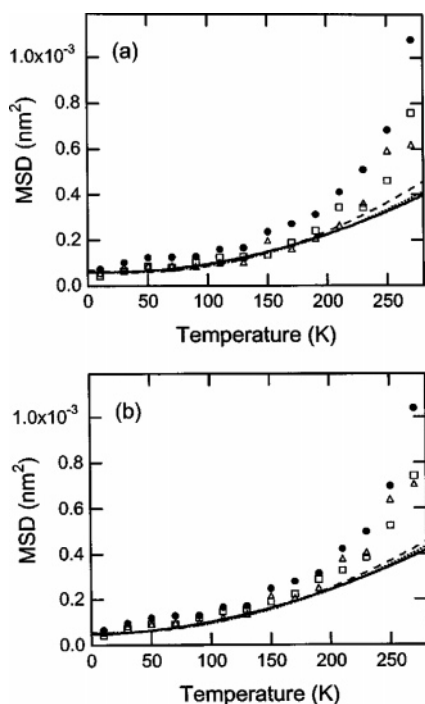


Figure 3. Temperature dependence of the mean-square displacement (MSD) of (a) oxygen and (b) hydrogen atoms in the ice lattice. The open squares, open triangles, and solid circles are the average MSD of the outermost bilayer of the basal surface along the in-plane *a* and *b* axes and the out-of-plane *c* axis, respectively. The dotted, dashed, and solid lines show the MSD of ice bulk along the in-plane *a* and *b* axes and the out-of-plane *c* axis, respectively (from ref 16).

a relatively thick quasi-liquid layer between the tip and the solid ice. The conversion from the solid ice to the quasi-liquid can happen at relatively lower pressures. The penetration speed is limited by the flow-out rate determined by the viscosity of the quasi-liquid layer.

These AFM indentation experiments also indicated that, if there is a quasi-liquid layer under the AFM tip, the viscosity of the quasi-liquid layer must be 2 orders of magnitude greater than that of bulk supercooled water. This substantial increase of viscosity may be due to the confinement of the quasi-liquid

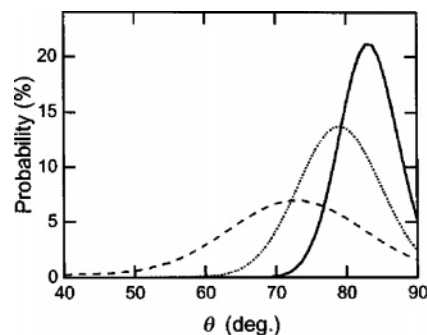


Figure 4. Distribution of the angle θ which the free O–H bond makes with the surface normal at 270, 130, and 10 K (the dashed, dotted, and solid curves, respectively, from ref 16).

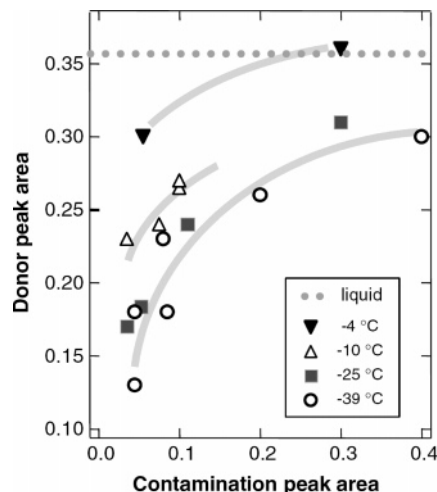


Figure 5. Premelting of the ice surface as a function of temperature and hydrocarbon contamination. The area of the free-hydrogen peak at 535 eV relative to the integrated NEXAFS spectrum (which measures the amount of liquid) is plotted versus the contamination peak area (532.5 eV, also relative to the integrated NEXAFS spectrum). Premelting thus depends strongly on both temperature and hydrocarbon coverage. The horizontal dotted line indicates the area of the free-hydrogen peak for the liquid water (from ref 19).

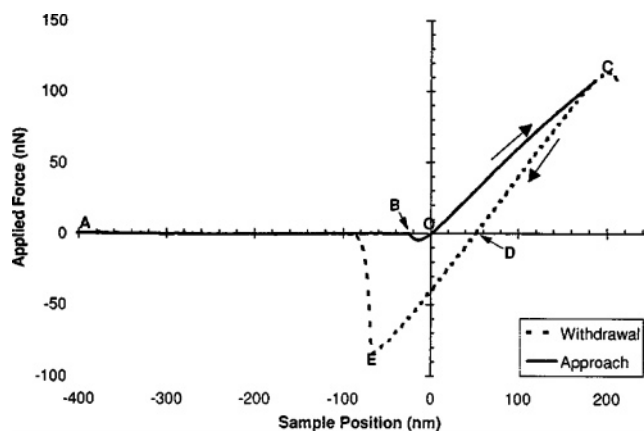


Figure 6. Typical force curve taken on 2/14/97 in 34 ms. The substrate temperature was -15.1 °C (from ref 37).

layer between the tip and the ice or the ordering structure of the quasi-liquid layer itself.

Lateral force microscopy is a promising technique for directly measuring the frictional properties on a microscopic scale. Using this technique, Bluhm et al. have measured the friction of ice films on mica substrates within a temperature range -24 to -40 °C.⁴⁰ In their experiment, the ice films were about 2 nm thick covered by a quasi-liquid layer of about 8 nm. Figure 8 shows

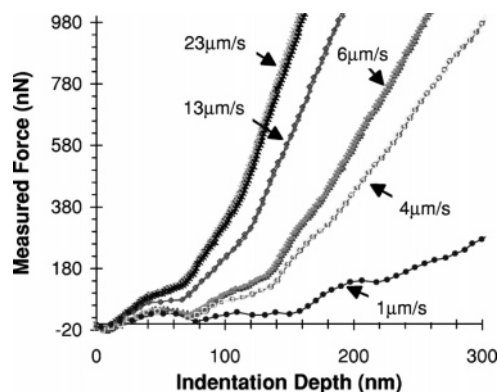


Figure 7. Measured force versus indentation depth at $-25.3\text{ }^{\circ}\text{C}$ and several sample velocities collected with a coated tip. The approximate indentation velocity at an indentation depth of 100 nm is given for each curve. Only the approach portion of each curve is shown (from ref 39).

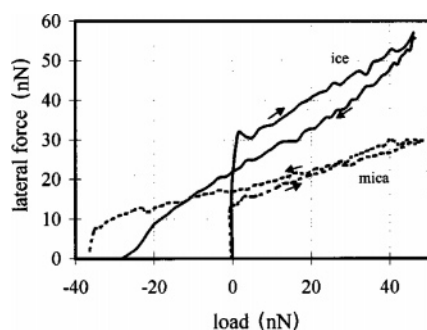


Figure 8. Lateral vs normal force curves for ice at $-24\text{ }^{\circ}\text{C}$ (solid line) and for mica at room temperature (dashed line). Arrows mark the curves for increasing and decreasing load. From the slopes of the linear portion of the curves, a “friction coefficient” for ice (0.6) and mica (0.3) can be obtained. The curves were taken using a triangularly shaped silicon cantilever with a normal spring constant of 0.4 N/m (from ref 40).

lateral versus normal force for the ice film at $-24\text{ }^{\circ}\text{C}$. From the slope of the linear portion of the curves in Figure 8, the “friction coefficient” is estimated to be about 0.6 for ice and 0.3 for mica. The friction coefficient of ice is about the same in the entire temperature region of their experiment and is always higher than that of mica. The estimated friction coefficient is comparable to the static friction of macroscopic measurements. This indicates that, in their experiment, the quasi-liquid layer was squeezed out and the tip was actually sliding on the dry ice. Another interesting observation in this experiment is that the friction coefficient on ice is higher than that on mica. This might be due to the breaking of hydrogen bonds during the tip sliding on ice.

Since the viscosity of the quasi-liquid layer is unknown, interpretations of aforementioned AFM-related experiments are based on the assumption whether a quasi-liquid layer exists between the tip and the ice or not. The viscosity of confined water can be measured by interfacial force microscopy (IFM). IFM is a force-controlled AFM which eliminates the jump-in instability problem of the conventional AFM and allows quantitative measurements of normal and lateral forces throughout the entire range of interfacial separation.⁴¹ A recent IFM study of confined water used a single-crystal Au(111) surface and an electrochemically etched Au tip.⁴² Each Au surface is made hydrophilic or hydrophobic by the chemisorption of a COOH or CH_3 terminated alkanethiol self-assembled monolayer (SAM). IFM results showed that the effective viscosity of water between two hydrophilic surfaces can be 7 orders of magnitude

greater than its bulk value when the water layer is about 0.6 nm thick. However, there is no significant increase of the viscosity of water between a hydrophobic surface and a hydrophilic (or hydrophobic) surface. The increase of viscosity has been attributed to the ordering increase in the confined water layer.

It will be interesting to perform an IFM study on the ice surface with hydrophobic and hydrophilic AFM tips. Measurement of the effective viscosity of the quasi-liquid layer may help us reveal the mechanism of plastic deformation and the frictional property of the ice surface. This study may also shed light on the question of how the unique molecular structure of the quasi-liquid layer affects its viscosity and makes itself macroscopically distinguishable from a water layer, which most of the current studies are not able to address directly.

Concluding Remarks and Outlook

Surface premelting is not unique to ice; it occurs on all types of solid. It is the ubiquity of ice in our universe that makes the premelting process on the ice surface become the origin of a wide range of important phenomena. As the temperature rises from absolute zero to the bulk melting point of ice, the surface structure and properties of ice change significantly (see Figure 9). These changes enable the ice surface to be actively involved in physical and chemical processes under different external conditions.

As shown by studies of surface structural properties, molecules in the surface layer of ice are very dynamic. Even at a temperature as low as 90 K, the large amplitude of vibrational motion of the first surface layer can make it invisible in the LEED surface crystallography. At temperatures around 200 K, the orientational disorder of the surface dangling OH bonds becomes detectable in the SFG spectrum. The mobility of surface molecules at an extremely low temperature is the direct consequence of the abrupt termination of the crystal bonding environment at the interface and the relatively weaker hydrogen bonding there. This phenomenon has also been verified in several molecular dynamics simulations.

At present, studies using various surface science techniques have confirmed the existence of the quasi-liquid layer on ice at temperatures below the bulk melting point and the layer thickening with increasing temperature. However, the temperature dependence of the premelting layer thickness and the viscosity of the quasi-liquid layer are not clearly determined. The uncertainties in various experimental results are mainly due to the use of different techniques to probe the premelting layer, the ice sample preparation procedures, and the contamination in the experimental environment. To improve the experiments, researchers have started to control sample preparation procedures better and to quantify the contamination effects both experimentally and theoretically.

It is commonly believed that the quasi-liquid layer is one of the major factors responsible for the extremely low friction of ice. Several microscopic indentation experiments have been performed to investigate the deformation of the ice surface under AFM tips. One of the interesting questions addressed is whether a quasi-liquid layer exists between the penetrating tip and the solid ice. Currently, indentation experiments suggest that, if there is a quasi-liquid layer, the viscosity of the quasi-liquid layer must be much greater than that of supercooled water. A lateral force microscopy experiment shows that, at a very low sliding speed and low temperatures, there is no quasi-liquid between the tip and the solid ice film and that the estimated friction coefficient is very high. In the future, further microscopic

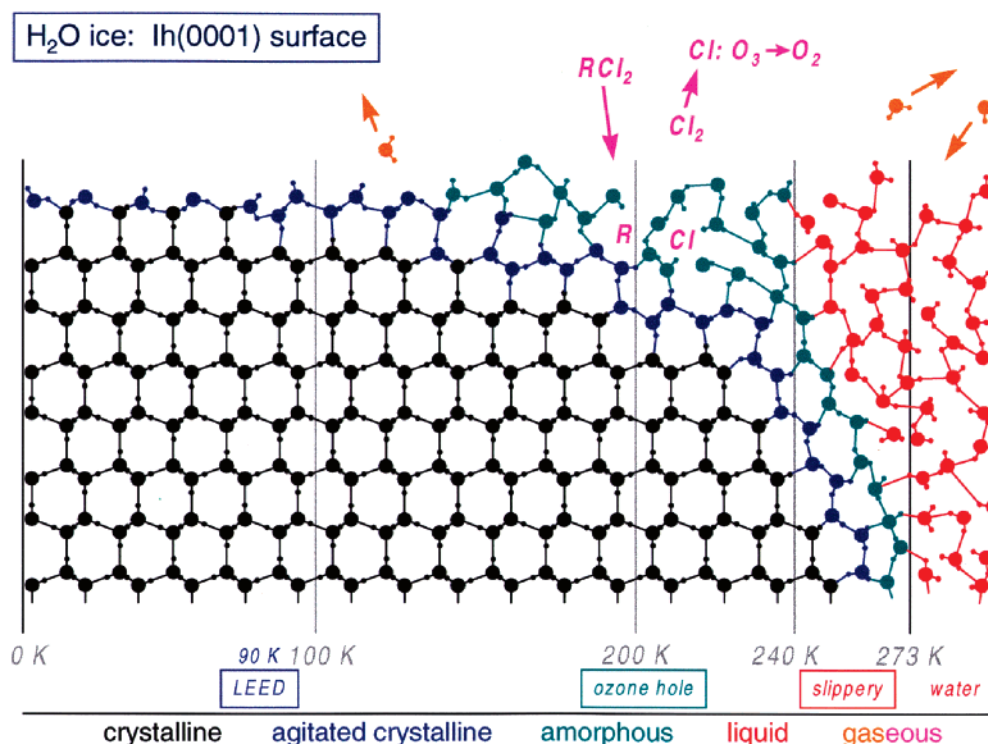


Figure 9. Proposed evolution of the surface structure of ice is shown as temperature rises from absolute zero (at left) to above the bulk melting point (273 K, at right). The LEED result (at 90 K), together with theory, suggests large vibrational amplitudes of the outermost water molecules still in the crystalline state (blue). As temperature rises, molecular agitation induces more crystalline defects, yielding an amorphous or quasi-liquid layer (green), as well as evaporation (orange). At about 190 K, ice in the Antarctic polar stratospheric clouds catalyzes Cl-containing molecules to Cl_2 , which in turn is dissociated by sunlight into Cl atoms that decompose ozone (O_3). The catalytic action may be due to the amorphous or quasi-liquid ice surface. Above about 240 K ($-30\text{ }^\circ\text{C}$, $-20\text{ }^\circ\text{F}$), the ice surface probably is liquid (red), to a thickness of 10 s to 100 s of Å. This permanent liquid film can explain the slipperiness of ice (by courtesy of Prof. Michel Van Hove).

TABLE 2: Surface Science Techniques for Measuring the Thickness of the Premelting Layer on Ice

surface technique	description	interface type	thickness at $-1\text{ }^\circ\text{C}$
proton channelling ¹⁶	detect thermal vibrations of the oxygen atoms in the premelting layer	vapor/ice (basal)	$\sim 94\text{ nm}$
ellipsometry ¹⁹	measure the dielectric profile at surface	vapor/ice (basal) vapor/ice (prism)	$\sim 5\text{ nm}$ $< 1.2\text{ nm}$
glancing-angle X-ray scattering ¹⁷	detect the disruption of the hydrogen-bonding network at surface	vapor/ice (basal)	30 nm
atomic force microscopy ²⁵	measure jump-in distance induced by the capillary force from the premelting layer	vapor/ice (prism) vapor/ice (polycrystalline)	$\sim 90\text{ nm}$ $\sim 20\text{ nm}$
near-edge X-ray absorption fine-structure spectra ²⁰	measure the intensity of transition from the O 1s core state to empty states which is affected by the bonding environment of water molecules at surface	vapor/ice (polycrystalline)	$\sim 2\text{ nm}$

investigations are expected to uncover how the quasi-liquid layer facilitates sliding on the ice surface.

Revealing environmental consequences of the surface premelting of ice is a major thrust for current research. The mobility of the premelting layer can facilitate the mass transport processes such as frost-heave in frozen soil, glacier motion, and the mass and charge transfer during collisions among ice particles in clouds. It was also suggested that, in polar stratospheric clouds, the premelting layer on ice particles can dissolve large amounts of inert chlorine and convert them into Cl_2 molecules whose photodissociation products, Cl atoms, decompose ozone. In these important environmental processes, the ice premelting layer is under complex external conditions. Thus, more detailed studies of surface premelting of ice are called for in order to fully understand its unique role.

Acknowledgment. This work was supported by the Director, Office of Science, Office of Advanced Scientific Computing

Research, Office of Basic Energy Sciences, Material Sciences and Engineering Division, of the U.S. Department of Energy under Contract No. DE-AC02-05CH11231.

References and Notes

- (1) Dash, J. G.; Fu, H. Y.; Wettlaufer, J. S. The premelting of ice and its environmental consequences. *Rep. Prog. Phys.* **1995**, 58 (1), 115–167.
- (2) Rosenberg, R. Why is ice slippery? *Phys. Today* **2005**, 58 (12), 50–55.
- (3) Dash, J. G.; Rempel, A. W.; Wettlaufer, J. S. The physics of premelted ice and its geophysical consequences. *Rev. Mod. Phys.* **2006**, 78 (3), 695–741.
- (4) Bowden, F. P.; Hughes, T. P. The mechanism of sliding on ice and snow. *Proc. R. Soc. London, Ser. A* **1939**, 172 (A949), 0280–0298.
- (5) Jellinek, H. H. Liquid-like (transition) layer on ice. *J. Colloid Interface Sci.* **1967**, 25 (2), 192.
- (6) Dash, J. G. History of the search for continuous melting. *Rev. Mod. Phys.* **1999**, 71 (5), 1737–1743.
- (7) Gilpin, R. R. Wire regelation at low-temperatures. *J. Colloid Interface Sci.* **1980**, 77 (2), 435–448.

- (8) Kouchi, A.; Furukawa, Y.; Kuroda, T. X-ray-diffraction pattern of quasi-liquid layer on ice crystal-surface. *J. Phys.* **1987**, *48* (C-1), 675–677.
- (9) Schick, M. *Introduction to Wetting Phenomena in Liquids at Interfaces*. Les Houches Lectures Session XLVIII; Charvolin, J., Joanny, J. F., Zinn-Justin, J., Eds.; Elsevier: New York, 1990.
- (10) Materer, N.; Starke, U.; Barbieri, A.; Van Hove, M.; Somorjai, G. A.; Kroes, G. J.; Minot, C. Molecular-surface structure of a low-temperature ice Ih(0001) crystal. *J. Phys. Chem.* **1995**, *99* (17), 6267–6269.
- (11) Materer, N. Molecular surface structure of ice (0001): Dynamical low-energy electron diffraction, total-energy calculations and molecular dynamics simulations. *Surf. Sci.* **1997**, *381* (2–3), 190–210.
- (12) Braun, J. Structure and phonons of the ice surface. *Phys. Rev. Lett.* **1998**, *80* (12), 2638–2641.
- (13) Glebov, A. A helium atom scattering study of the structure and phonon dynamics of the ice surface. *J. Chem. Phys.* **2000**, *112* (24), 11011–11022.
- (14) Wei, X.; Miranda, P. B.; Shen, Y. R. Surface vibrational spectroscopic study of surface melting of ice. *Phys. Rev. Lett.* **2001**, *86* (8), 1554–1557.
- (15) Wei, X. Sum-frequency spectroscopic studies of ice interfaces. *Phys. Rev. B* **2002**, *66* (8), 13.
- (16) Golecki, I.; Jaccard, C. Intrinsic surface disorder in ice near melting-point. *J. Phys. C: Solid State Phys.* **1978**, *11* (20), 4229–4237.
- (17) Dosch, H.; Lied, A.; Bilgram, J. H. Glancing-angle X-ray-scattering studies of the premelting of ice surfaces. *Surf. Sci.* **1995**, *327* (1–2), 145–164.
- (18) Ikeda-Fukazawa, T.; Kawamura, K. Molecular-dynamics studies of surface of ice Ih. *J. Chem. Phys.* **2004**, *120* (3), 1395–1401.
- (19) Beaglehole, D.; Nason, D. Transition layer on the surface on ice. *Surf. Sci.* **1980**, *96* (1–3), 357–363.
- (20) Bluhm, H. The premelting of ice studied with photoelectron spectroscopy. *J. Phys.: Condens. Matter* **2002**, *14* (8), L227–L233.
- (21) Bluhm, H.; Salmeron, M. Growth of nanometer thin ice films from water vapor studied using scanning polarization force microscopy. *J. Chem. Phys.* **1999**, *111* (15), 6947–6954.
- (22) Furukawa, Y.; Yamamoto, M.; Kuroda, T. Ellipsometric study of the transition layer on the surface of an ice crystal. *J. Cryst. Growth* **1987**, *82* (4), 665–677.
- (23) Elbaum, M.; Lipson, S. G.; Dash, J. G. Optical study of surface melting on ice. *J. Cryst. Growth* **1993**, *129* (3–4), 491–505.
- (24) Dosch, H.; Lied, A.; Bilgram, J. H. Disruption of the hydrogen-bonding network at the surface of I-h ice near surface premelting. *Surf. Sci.* **1996**, *366* (1), 43–50.
- (25) Doppenschmidt, A.; Butt, H. J. Measuring the thickness of the liquid-like layer on ice surfaces with atomic force microscopy. *Langmuir* **2000**, *16* (16), 6709–6714.
- (26) Kaverin, A.; Tsionsky, V.; Zagidulin, D.; Daikhin, L.; Alengoz, E.; Gileadi, E. A novel approach for direct measurement of the thickness of the liquid-like layer at the ice/solid interface. *J. Phys. Chem. B* **2004**, *108* (26), 8759–8762.
- (27) Lied, A.; Dosch, H.; Bilgram, J. H. Surface melting of ice I(h) single-crystals revealed by glancing angle X-ray-scattering. *Phys. Rev. Lett.* **1994**, *72* (22), 3554–3557.
- (28) Sadtschenko, V.; Ewing, G. E. A new approach to the study of interfacial melting of ice: infrared spectroscopy. *Can. J. Phys.* **2003**, *81* (1–2), 333–341.
- (29) Wettlaufer, J. S. Impurity effects in the premelting of ice. *Phys. Rev. Lett.* **1999**, *82* (12), 2516–2519.
- (30) Ikeda-Fukazawa, T.; Kawamura, K. Effects of ions on dynamics of ice surface. *Chem. Phys. Lett.* **2006**, *417* (4–6), 561–565.
- (31) Evans, D. C. B.; Nye, J. F.; Cheeseman, K. J. The kinetic friction of ice. *Proc. R. Soc. London* **1976**, *347* (1651), 493–512.
- (32) Persson, B. N. J. *Sliding friction: physical principles and applications*, 2nd ed.; Springer: New York, 2000.
- (33) Colbeck, S. C.; Najarian, L.; Smith, H. B. Sliding temperatures of ice skates. *Am. J. Phys.* **1997**, *65* (6), 488–492.
- (34) Dekoning, J. J.; Degroot, G.; Schenau, G. J. V. Ice friction during speed skating. *J. Biomech.* **1992**, *25* (6), 565–571.
- (35) Barnes, P.; Tabor, D. Plastic flow and pressure melting in deformation of ice I. *Nature* **1966**, *210* (5039), 878–880.
- (36) Barnes, P.; Tabor, D.; Walker, J. C. F. Friction and creep of polycrystalline ice. *Proc. R. Soc. London: Ser. A* **1971**, *324*(1557), 127.
- (37) Pittenger, B. Investigation of ice-solid interfaces by force microscopy: Plastic flow and adhesive forces. *J. Vac. Sci. Technol., A* **1998**, *16* (6), 3582–3582.
- (38) Butt, H. J. Analysis of plastic deformation in atomic force microscopy: Application to ice. *J. Chem. Phys.* **2000**, *113* (3), 1194–1203.
- (39) Pittenger, B. Premelting at ice-solid interfaces studied via velocity-dependent indentation with force microscope tips. *Phys. Rev. B* **2001**, *63*(13), 13.
- (40) Bluhm, H.; Inoue, T.; Salmeron, M. Friction of ice measured using lateral force microscopy. *Phys. Rev. B* **2000**, *61* (11), 7760–7765.
- (41) Joyce, S. A.; Houston, J. E. A New Force Sensor Incorporating Force-Feedback Control for Interfacial Force Microscopy. *Rev. Sci. Instrum.* **1991**, *62* (3), 710–715.
- (42) Major, R. C. Viscous water meniscus under nanoconfinement. *Phys. Rev. Lett.* **2006**, *96* (17), 17.